FEMTOCHEMISTRY and FEMTOBIOLOGY

Ultrafast Events in Molecular Science

VIth International Conference on Femtochemistry
Maison de la Chimie, Paris, France
July 6-10, 2003

Edited by

Monique M. Martin*
and
James T. Hynes*/**

**UMR CNRS-ENS 8640, PASTEUR*
Department of Chemistry, Ecole Normale Supérieure
24 rue Lhomond, 75231 Paris Cedex 05, France
and
***Department of Chemistry and Biochemistry*
University of Colorado
Boulder, CO 80309-0215, USA

2004

ELSEVIER
Amsterdam – Boston – Heidelberg – London – New York – Oxford – Paris
San Diego – San Francisco – Singapore – Sydney – Tokyo

Femtochemistry and Femtobiology
M.M. Martin and J.T. Hynes (editors)

Time-resolved x-ray diffraction from small molecules in solution

M. Wulff[a], M. Lorenc[a], A. Plech[b], H. Ihee[c], S. Bratos[d], F. Mirloup[d] and R. Vuilleumier[d]

[a]European Synchrotron Radiation Facility, Grenoble Cedex 38043, BP 220, France

[b]Fachbereich Physik der Universitaet Konstanz, Universitaetsstrasse 10, D-78457 Konstanz, Germany

[c]Department of Chemistry (School of Molecular Science - BK21), Korea Advanced Institute of Science and Technology, Daejeon, 305-701, Republic of Korea

[d]Laboratoire de Physique Théorique des Liquides, Université Pierre et Marie Curie, Case courrier 121, 4, Place Jussieu, Paris Cedex 75252, France

We describe beamline ID09B at the European Synchrotron Radiation Facility (ESRF), a laboratory for optical pump and x-ray probe experiments to 100-picosecond resolution. The x-ray source is a narrow-band undulator, which can produce up to 1×10^{10} photons in one pulse. The 3% bandwidth of the undulator is sufficiently monochromatic for most diffraction experiments in liquids. A Ti: sapphire femtosecond laser is used for reaction initiation. The laser runs at 896 Hz and the wavelength is tunable between 290-1160 nm. The doubled (400 nm) and tripled wavelength (267 nm) are also available. The x-ray repetition frequency from the synchrotron is reduced to 896 Hz by a chopper. The time delay can be varied from 0 ps to 1 ms, which makes it possible to follow structural processes occurring in a wide range of time scales in one experiment.
We present a preliminary study on the structural dynamics of photo-excited iodine in methanol. At early time delays after dissociation, 1 – 10 ns, the change in the diffracted intensity $\Delta S(q, \tau)$ is oscillatory and the high-q part 4 –8 $Å^{-1}$ is assigned to free iodine atoms. At later times, 10-100 ns, expansive motion is seen in the bulk liquid. The expansion is driven by energy released from the recombination of iodine atoms. The $\Delta S(q, \tau)$ curves between 0.1 and 5 μs coincide with the temperature differential dS/dT for static methanol with a temperature rise of 2.5 K. However, this temperature is five times greater than the temperature deduced from the energy of dissociated atoms at 1 ns. The discrepancy is ascribed to a short-lived state that recombines on the sub-nanosecond time scale.

1. INTRODUCTION

The high intensity of x-ray beams from modern synchrotrons has made it possible to conduct optical pump and x-ray probe experiments to a time resolution of 100 ps, i.e. the limit given by the x-ray pulse length of a synchrotron. In these machines, the brightest

beams are produced by undulators. An undulator is an array of magnets that produce an oscillating magnetic field in a straight section of the synchrotron. The magnetic field forces the electrons into a "slalom"-like motion. Polychromatic flashes of x-rays are produced at the turning points, and the emission from successive turning points interferes. The interference frequency, or x-ray frequency, is determined by the time it takes for an electron to run through one period in the orbit [1]. The interference boosts the intensity at the given frequency and the spectral bandwidth becomes narrower [2]. Note that the interference is a *single-electron* effect, i.e. the emission from several electrons in a bunch adds incoherently. The spectrum of the U17 undulator in beamline ID09B at the ESRF is shown in Fig. 1. The figure gives the spectral flux produced by one bunch of 2 x 10^{11} electrons.

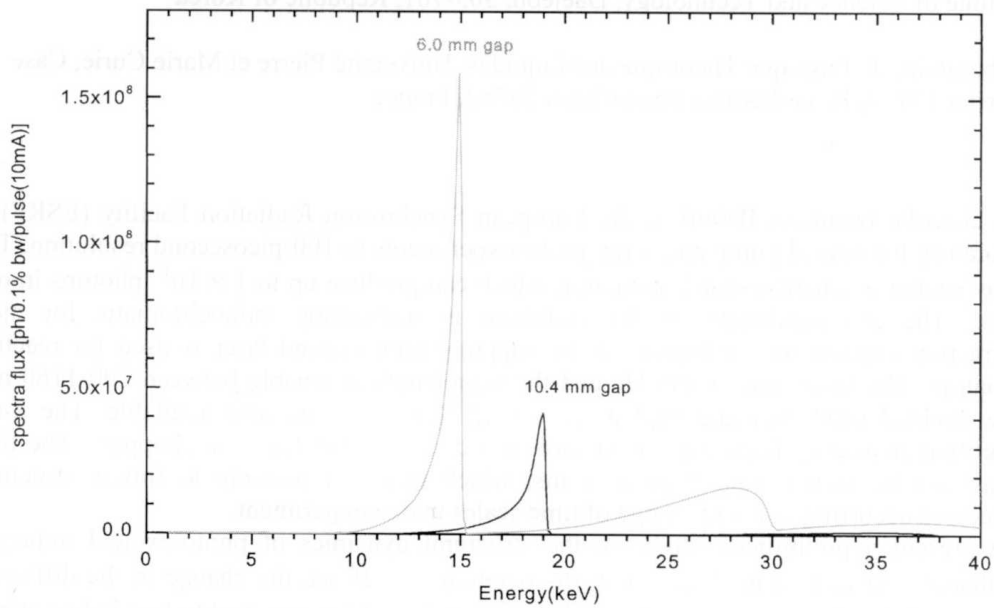

Fig. 1. Spectra from the U17 undulator .The red curve is the 6.0 mm gap spectrum used for Laue diffraction from proteins and the black curve, the 10.4 mm gap spectrum used for liquid experiments.

The weakest point in synchrotron work is the relatively poor time resolution of 100 ps. This time scale is $10^3 - 10^4$ longer than the chemical time scale set by the formation and breakage of bonds. Laser-driven plasma sources can generate sub-picosecond x-ray pulses, but their 4π emission makes it difficult to focus more than 5×10^4 photons per pulse on a small sample. That restricts its application to strongly scattering samples, for example, Bragg diffraction from laser-excited surfaces of semiconductors. Non-thermal melting was recently studied using a plasma source [3]. The X-ray Free Electron Laser (XFEL) will eventually produce 100 fs x-ray pulses of tremendous intensity and spectral purity, but we

will have to wait until 2008 for the first prototype, which is being designed at SLAC in Stanford (the LCLS project).

An alternative structural probe is electron diffraction, which can be used to measure the structural change of gas molecules. The time resolution of this technique may be as low as a few picoseconds. In Table 1, we compare electron diffraction to x-ray diffraction. The relative scattering cross-section of electrons is about million times higher than that of x-rays [4]. This makes electron diffraction the method of choice for gas-phase studies [5]. Fortunately, one can make up for the deficiency by increasing the x-ray flux. Thus, a state-of-the-art DC electron gun can generate ~10^4 electrons in a bunch with a pulse length of a few picoseconds [5], while the ID09B beamline can produce ~10^9-10^{10} x-ray photons per pulse. Therefore, with the same repetition rate, the overall scattering power of electrons is 10 to 100 times higher than that of x-rays. However, the number of solute molecules in time-resolved x-ray diffraction in solution is 10 to 1000 times higher than that in ultrafast electron diffraction in the gas phase, thus resulting in the same overall signals from solute molecules. One big difference is that the gas-phase sample in electron diffraction is free from the background from the solvent, which constitutes the major part of the total signal in a liquid. This huge background complicates the data processing and analysis, but in the end, it gives us valuable information about the solvent change, which is absent in gas-phase electron diffraction. The consequence of the high scattering cross section of electrons is its low penetration depth, which makes difficult the application of electron diffraction to typical liquid samples. By comparison, prospective parameters for the future XFEL (TESLA) is also listed and one can see that XFEL will provide at least 10 times more signal with femtosecond time resolution.

Table 1
Comparison between ultrafast electron diffraction (UED), x-ray diffraction (UXD), and the prospective X-ray Free Electron Laser (XFEL)

	UED	UXD	XFEL
Relative scattering power	10^6	1	1
Number of scattering particles	4×10^4 / pulse	10^9 / pulse	10^{12} / pulse
Repetition rate	1 kHz	900 Hz	10 Hz
Overall scattering power	10 ~ 100	1	10
Number of solute molecules	~10^{11}	10^{12} ~ 10^{14}	10^{12} ~ 10^{14}
Overall relative signal from solute	1	1 ~ 10	10 ~ 100
Background from solvent	none	huge	huge
Pulse width	1-5 ps	60-120 ps	100 fs
q-range	1.5 – 18.5 Å^{-1}	0.2 – 15 Å^{-1}	0.2 – 15 Å^{-1}

We have used x-ray diffraction in our laboratory to probe transient structures of laser-excited liquids, small-molecule crystals and protein crystals. The diffraction patterns are recorded on a CCD detector that makes efficient use of most of the diffracted x-rays. Several experimental protocols have been developed: Laue diffraction from proteins [6-8], small-molecule diffraction [9,10] and diffraction from liquids [2,11,12]. In proteins, the

narrow-bandwidth Laue method has greatly improved the data quality and outclassed the traditional wiggler approach [13]. As a new application, Laue diffraction was recently used in a study of laser excited iodine in CCl_4 where the 3% bandwidth provides a good compromise between q-resolution and flux. This is due to the natural positional and orientational dispersion in a liquid [14]. The exposure time in a liquid experiment is typically 10 seconds, 500-1000 times shorter than an equivalent monochromatic exposure. As a result, we can now collect complete structural data of a chemical reaction in solution in 2 – 3 hours per sample. We will briefly describe the x-ray source and its optics.

2. THE X-RAY SOURCE

The straight sections in the ESRF storage ring can accommodate three 1.6-m long in-air undulators, or two 2.0-m long in-vacuum undulators. The in-air undulators operate at 11.0-mm gap, the in-vacuum undulators at 6.0 mm. In the in-vacuum undulator, the magnets are brought much closer to the electron beam. That increases the magnetic field and hence the acceleration of the electrons. With an in-vacuum undulator in a high-energy synchrotron as the ESRF, it is possible to raise the fundamental energy to 15-20 keV with fairly weak higher harmonics, see Fig. 1. This mono-harmonic feature comes at the expense of tunability (low K). The fundamental of the U17 devise is 15.0 keV (0.83 Å) at 6 mm gap and 20.3 keV at 20 mm gap. The undulator parameters are shown in table 2. The U46 in-air undulator will be replaced in January 2005 by a U20 in-vacuum undulator, with a fundamental energy of 9.0 keV.

Table 2
Undulator parameters as of October 2003. E_f is the undulator fundamental, E_c the critical energy of the bending magnet radiation in the "slalom" motion.

period (mm)	poles	minimum gap (mm)	B_{max} (T)	E_f (keV)	E_c (keV)	K	P (W/200 mA)
17	236	6.0	0.544	15.03	13.2	0.86	450
46	71	16.0	0.643	0.64	15.6	2.76	289

3. THE X-RAY OPTICS

The first optical element in the raw polychromatic beam is the channel-cut monochromator. It is a two-bounce monochromator cut from a monolithic piece of silicon. The diffracting surface is (111) which gives a band pass $\delta E/E = 1.4 \times 10^{-4}$. The energy can be varied between 4 – 50 keV. The next element is the cylindrical focusing mirror. Gravity bends the mirror into a toroid with a meridional curvature of 9.9 km, which is needed to focus on the sample, 22 m downstream. The incidence angle is 2.722 mrad. The mirror surface is coated with platinum that reflects in the range 0 – 27 keV. The meridional curvature is fine tuned by a stepper motor acting from below the mirror. The slope-error of the optical surface is as low as 0.67 μrad (rms) in the 450-mm central zone. That gives a focal spot as small as 0.10 x 0.06 mm^2 in the horizontal and vertical direction respectively.

Finally we are installing second monochromator based on multilayer optics (ML). The aim is to make better use of the polychromatic spectrum from the undulator. By varying the Bragg angle of the second ML, the bandwidth can be tuned between 0.2 – 2.0%. It will be installed side by side with the channel-cut monochromator. The multilayers are deposited on flat blocks of silicon with a slope error of 0.4 μrad (rms). The system will be cryogenically cooled. There will be two ML stripes with the compositions Ru/Al_2O_3 (d = 40Å, 10-20keV) and Ir/Al_2O_3 (d = 25.5 Å, 20-32 keV). The ML optics will also suppress the second harmonic. Note that ML optics together with the U20 undulator will give access to the polychromatic beam from higher harmonics of the undulators, which otherwise can not be used in polychromatic experiments. The q range will increase from 9 to 15 $Å^{-1}$. The flux numbers are shown in Table 3.

Table 3
Flux numbers for pump and probe experiments at 15 keV (U17).

Beamline configuration	Single-pulse flux ph/pulse (10mA)	Flux at 896.6 Hz ph/s (10mA)
Mirror (white beam)	1.1×10^{10}	9.6×10^{12}
Multilayers + mirror	1.7×10^{9}	1.5×10^{12}
Monochromator + mirror	2.4×10^{7}	2.2×10^{10}

4. THE RECOMBINATION OF IODINE IN SOLUTION

As an example of a time resolved diffraction experiment, we will describe the dissociation and recombination of molecular iodine in solution using the standard model developed by Harris [15] and others. The interaction energy of two iodine atoms in the gas phase is shown in Fig 2. If the solvent is chemically inert, as in the case of CCl_4, this potential is a good starting point. The I_2 molecule is first excited to a mixture of the B and $^1\pi_u$ state by a pulse of green light (530 nm, 2.340 eV, 150 fs). Calculations of the transition matrix elements show that the B and $^1\pi_u$ states are populated as 5.2 : 1 [16]. Both curves are initially repulsive and the molecule moves apart. After a few collisions in the cage, the majority of atoms recombine (geminate recombination); others escape as atoms. The separated atoms recombine diffusively in 10-100 ns (non-geminate recombination). The collisions with the cage cool the excited molecules and the molecules relax towards the minima on either the X or the A/A' curve. The molecules that relax along the X potential are cooled in a process called vibrational cooling, which takes 50 – 200 ps depending on the solvent. The A/A' molecules relax to a meta-stable state with a bond length of 3.0 Å. The lifetime of the A/A' state depends on the polarity of the solvent; it varies from 60 ps in alkane solvents to 2.7 ns in CCl_4. We expect that the A/A' state decays to the ground state via collisions with the solvent that expand the molecule to the cage boundary. Here the energy-gap to the ground state is smaller which facilitates curve crossing to the ground state [17,18].

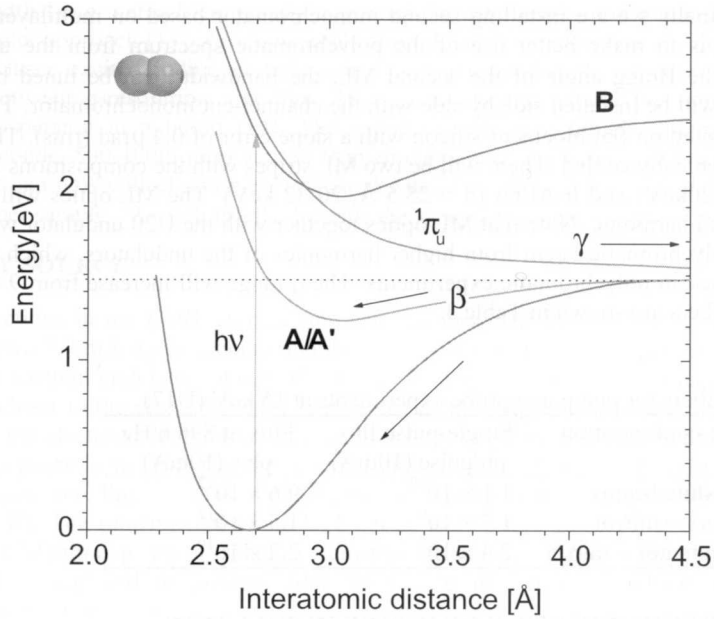

Fig. 2. The energy of two iodine atoms as a function of their distance.

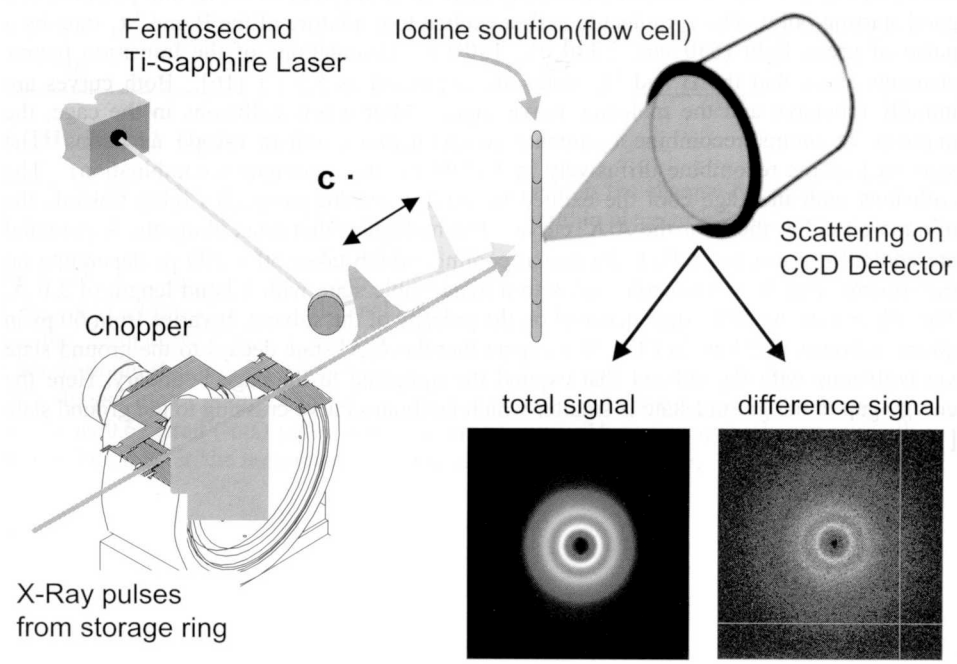

Fig.3. The laser pump and x-ray pump set-up on beamline ID09B.

The diffracted intensity from the solute and the solvent is recorded on a CCD detector in an angular dispersive way, see Fig. 3. The detector is a 16-bit MARCCD with a diameter of 132 mm. The intensity $S_{tot}(q,\tau)$ is measured as a function of the scattering vector q and the time delay τ. Note that $q = 4\pi\sin(\theta)/\lambda$, where 2θ is the scattering angle and λ the x-ray wavelength. The intensity has two contributions: elastic scattering (diffraction) $S_{elas}(q,\tau)$ and inelastic Compton scattering $S_{inelas}(q,\tau)$. The Compton scattering is an atomic property, and thus independent of changes in molecular structure [19,20]. Consequently the Compton contribution cancels out in the difference, i.e. $\Delta S_{tot}(q,\tau) = \Delta S_{elas}(q,\tau)$ for patterns with and without laser excitation.

The diffracted intensity from a molecule in the gas phase is expressed by the Debye Equation [21]:

$$S(q) = I_0 \, r_0^2 \, P \sum_{n,m} f_n(q) \, f_m(q) \frac{\sin(q \, r_{nm})}{q \, r_{nm}}.$$

Here I_0 is the intensity of the x-ray beam, $r_0 = e^2/mc^2$ is the classical electron radius (2.82 x 10^{-15} m). $P(\theta,\phi)$ is the polarization of the x-rays; it depends on the angle between the polarization and the scattering vector. For horizontally polarized x-rays, it takes the form $P(\theta, \phi) = 1 - \sin^2 2\theta \, \sin^2\phi$, where 2θ is the scattering angle and ϕ the azimuthal angle with respect to the vertical direction. The formfactor $f(q)$ is the Fourier transform of the atomic electron density:

$$f(q) = \int_0^\infty 4\pi \, r^2 \, \rho(r) \frac{\sin(q \, r)}{q \, r} dr.$$

We note that the sum above is over all pairs of atoms in the molecule and that the intensity decreases as r_{ij}^{-1}; the interference length is relatively long-range. The scattered intensity in the forward direction q = 0 reduces to:

$$S(q = 0) = I_0 \, r_0^2 \, (\sum Z_n)^2,$$

where Z_n is the number of electrons in atom n. The forward scattering is the coherent scattering from all the electrons in the molecule. If we consider the reaction $I_2 \rightarrow 2\ I$, the difference intensity between dissociated and non-dissociated states is proportional to $2Z^2 - 4Z^2 = -2Z^2$. The negative intensity change in the forward scattering is normally the signature of dissociation.

The intensity from a diatomic molecule is:

$$S(q) = 2 I_0 \, r_0^2 \, P(\theta,\varphi) f_I^{\,2}(q) \left(1 + \frac{\sin(q \, r(I-I))}{q \, r(I-I)}\right),$$

where r(I-I) is the bondlength 2.666 Å of gas-phase iodine. The first stage in the data analysis is usually to fit the high-q difference data to a gas-phase expression for the molecular change (see later).

The concentration of iodine should be optimized, if possible, to give the highest possible signal to noise in the difference pattern. If we neglect x-ray absorption (thin sample & high x-ray energy) and if the laser absorption follows Beer-Lambert's law (no saturation), one can show that the optimal signal to noise is obtained for an optical density

OD of ~ 0.55 for a parallel geometry of the laser and x-ray beams. By definition, OD = $\varepsilon \cdot c \cdot t$, where ε is the molar-extinction-coefficient at the excitation wavelength, c the concentration and t the sample thickness. If iodine is excited at the peak of the absorption band at 530 nm, $\varepsilon = 81 \times 10^3$ liter/mole/m, $t = 3 \times 10^{-4}$ m, the optimal concentration is c = 0.022 mole/liter. The concentration of liquid CCl_4 is 10.4 mole/liter. That gives a ratio of I_2 to CCl_4 of 1: 471. This highlights the prime difficulty in liquids: the signal to background is always small and that requires an intense x-ray beam. In a recent study of I_2 in CCl_4, the difference signals were 10^{-2}-10^{-4} of the solvent background.

We will now examine the difference spectra from iodine in methanol (CH_3OH) at 75 mM concentration. Iodine makes a charge transfer with oxygen [22], and the excited-state structure is not known. The charge transfer shifts the absorption peak from 530 nm to 445 nm. In practice we can excite the complex with 400 nm light from the second harmonic of the Ti: sapphire laser. Note that the solvent background is fairly weak due to its low effective Z value. The U17 undulator was operated at 9.0 mm gap at a fundamental energy of 18.2 keV. The spectrum was measured and the effective energy of the experiment calculated as the centre of mass (COM) of the photon-energy distribution. The COM calculation includes all known absorptions (windows, air, capillary, sample and detector). That gives an E_{COM} of 17.55 keV (0.706Å). The x-rays were focused to 0.10×0.06 mm^2 and the slits before the sample set to 0.10×0.07 mm^2. The flux on the sample was 2×10^{11} ph/s and the exposure time ~ 5 s per frame. The liquid sample was pumped though the focal point in a capillary and the flow speed adjusted to have a fresh sample for every new x-ray pulse. The ground state of the sample was recorded as a negative time delay (reference) at -3ns. The CCD images were collected in pairs of negative (reference) and positive time delays in order to check for drifts. The exposure time was scaled to the synchrotron current; the detector was always exposed to the same level. The detector was placed 42.5 mm from the sample and the scattering angle recorded between $2 < 2\theta < 56°$.

The CCD image from the ground state of I_2 in methanol is shown in Fig. 4. Note the beamstop in the center (black area) and the yellow cone of scattering from methanol. The x-ray polarization is evident from the elongated diffraction pattern. The picture to the right is the difference image for a time delay of 100 ps. Note the black ring surrounding the beamstop and the whiter ring at higher angles. The dark ring is the negative signal from free I atoms. The radial intensity is shown in Fig. 5 for 100 ps and 1 μs. Note that the scattering changes sign after 1 μs at small q. The 1 μs curve is the unambiguous signature of expansion in the solvent host. The expansion is driven by the energy released by recombining iodine. The expansion is not an artifact of laser heating; it is an intrinsic feature from the recombination of iodine atoms in a liquid, and therefore cannot escape diffraction measurement.

The difference amplitude $\Delta S_{elas}(q,\tau)$ can be expressed in absolute units by scaling to the methanol background. The difference curves can thus be written in units of the classical electron radius r_0^2 per CH_3OH molecule. The high-q part of the difference curves between 1 - 10 ns is readily fitted to the difference in Debye scattering between I_2 and 2I. We thus believe that atomic scattering is the dominant contribution to the signal between 1 - 10 ns. The analysis shows that 4% of the I_2 molecules are excited at 1 ns. Now, given that each excited molecule receives hν of energy from the laser, we can calculate the temperature rise

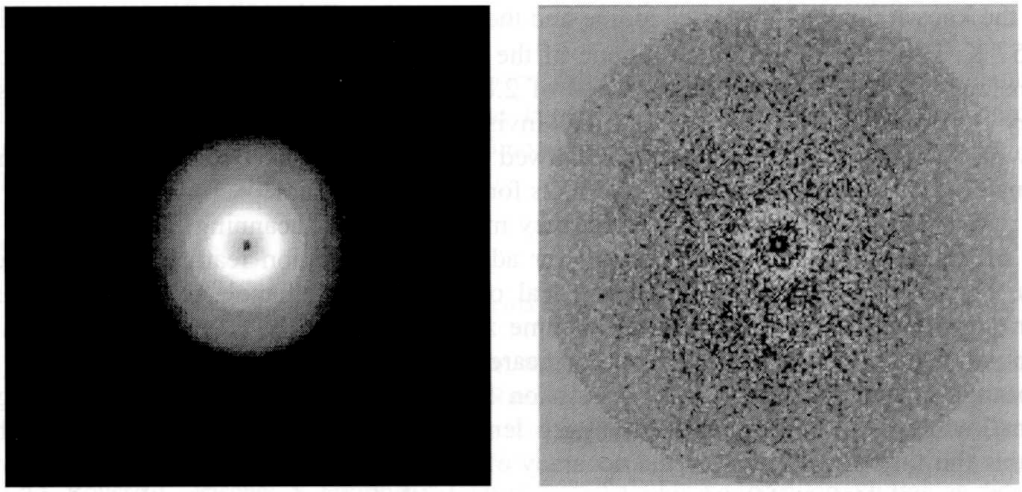

Fig. 4. The diffraction pattern from the ground state of iodine in methanol is shown on the right. The beamstop is seen as a dark circular area in the centre and the bright ring is the correlation peak from the liquid. The picture on the right is the subtraction of the ground state from the 100 ps frame. Note the black ring around the beamstop. That is the signature of dissociation.

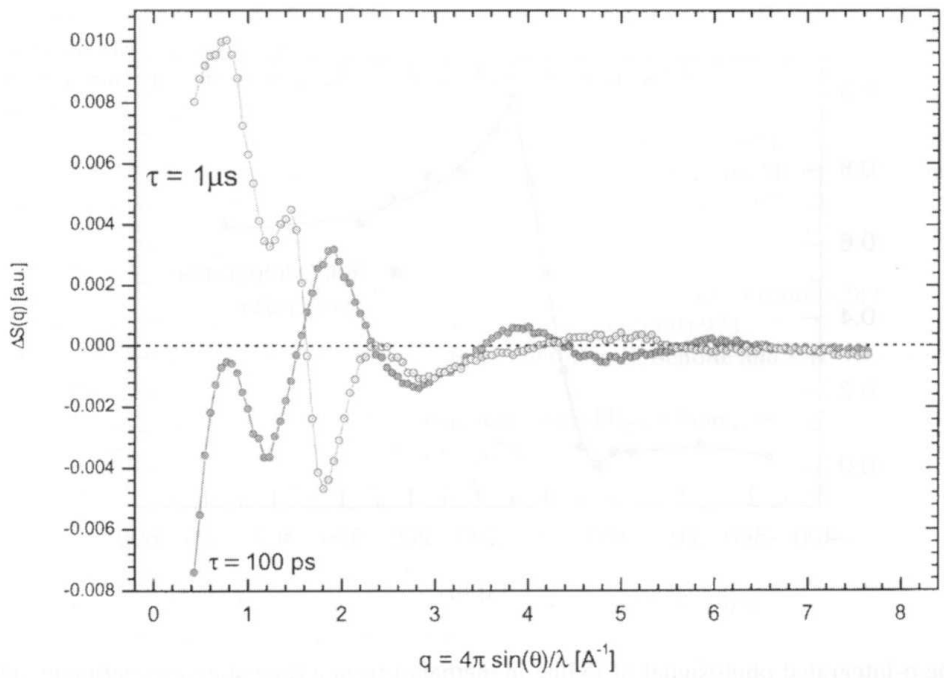

Fig. 5. The laser induced change in the radially averaged scattering intensity. The curves have been scaled to the intensity of the liquid background at Q = 5.76 Å.

from the known density of excited iodine and the heat capacity. We infer a temperature rise of 0.57 K. However, from the amplitude of the 1 μs time point, i.e. the magnitude of the expansion, we deduce a temperature rise of 2.8 K. This indicates that 80% of the laser energy is absorbed into processes that are "invisible" in the 1-10 ns data. This result is in line with the study of I_2 in CCl_4, which showed that 87% of the excited iodine recombines geminately [12]. We have seen similar effects for HgI_2 in methanol.

We have investigated this discrepancy more closely by scanning the laser pulse in steps of 25 ps though time-zero to look for additional oscillation features at the earliest times. Fig. 6 shows the average photosignal of iodine in methanol from a fine slicing experiment. This shows the definition of time zero, which can be derived from the data. The black line is a fit of the instant onset smeared out by the temporal response function of the beamline. The derivative of this function is a gaussian with a 110 ps pulse length (fwhm), which is consistent with the bunch length measurement from the machine. This explains the time resolution and the accuracy of the experiment. It turns out that the total intensity is greatest at 50 ps which may indicate that we are seeing the tail of the exponential decay of the A/A' state (Fig. 6). However the q-dependence of the 100 ps curve does not fit that of a simple inflated I_2 molecule if we constrain the bond lengths to 3.0-3.5 Å. This may be the signature of a A/A'-state complex with methanol, or a A/A' state caged by methanol and we plan to investigate this problem in more details by incorporating Molecular Dynamics simulations, which may account for the solute/solvent interaction in a qualitative way.

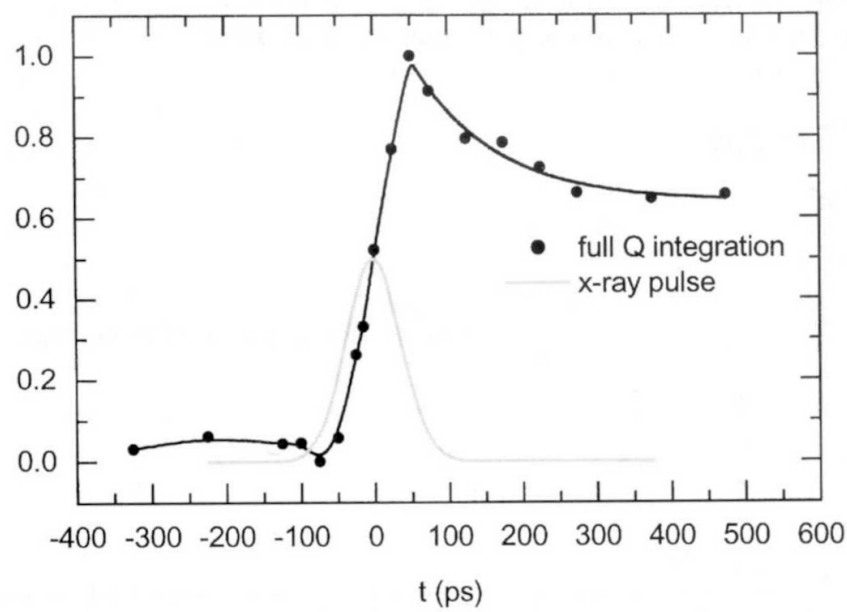

Fig. 6. The q-integrated photosignal of iodine in methanol from a time-slicing experiment. The red curve is the temporal profile of the x-ray pulse.

ACKNOWDLEDGEMENT

The authors wish to thank Laurent Eybert, Laurent Claustre, Wolfgang Reichenbach, Richard Neutze, Armin Geis, Dominique Block and Peter Trommsdorff for help and discussions. Finally we would like to acknowledge financial support from the EU-grant HPRI-CT-0415.

References

[1] J. Als-Nielsen and D. Mc Morrow. Elements of modern x-ray physics, J. Wiley & Sons, New York, 2001.
[2] F. Schotte, S. Techert S, P. A. Anfinrud, V. Srajer, K. Moffat and M. Wulff. Recent Advances in the Generation of Pulsed Synchrotron Radiation Suitable for Picosecond Time-resolved X-ray Studies. Third-Generation Hard X-ray Synchrotron Radiation Sources. Edited by Dennis Mills, (ISBN 0-471-31433-1). 345-401, 2002
[3] A. Rousse, C. Rischel, S. Fourmaux, I. Uschmann, S. Sebban, G. Grillon, Ph Balcou, E. Forster, J.P. Geindre, P. Audebert, J.C. Gauthier and D. Hulin, Nature, 410 (2001) 65.
[4] M. H. Pirenne, The Diffraction of X-rays and Electrons by Free Molecules, The University Press, Cambridge, 1946.
[5] H. Ihee, V. A. Lobastov, U. M. Gomez, B. M. Goodson, R. Srinivasan, C. Y. Ruan, A. H. Zewail, Science, 291 (2001) 458
[6] V. Srajer, T. Teng, T. Ursby, C. Pradervand, Z. Ren, S. Adachi, W. Schildkamp, D. Bourgeois, M. Wulff and K. Moffat, Science, 274 (1996) 1726.
[7] B. Perman, V. Srajer, Z. Ren, T-Y. Teng, C. Pradervand, T. Ursby. F. Schotte, M. Wulff, R. Kort, K. Hellingwerf and K. Moffat, Science, 279 (1998) 1946.
[8] F. Schotte, M. Lim, T. A. Jackson, A. V. Smirnov, S. Jayashree, J.S. Olson, G. N. Phillips, M. Wulff, P. A. Anfinrud, Science, 300 (2003) 1944.
[9] S. Techert, F. Schotte and M. Wulff, Phys. Rev. Lett., 86 (2001) 2030.
[10] E. Collet, M. H. Lemée-Cailleau, M. Buron-Le Cointe, H. Cailleau, M. Wulff, T. Luty, S. Y. Koshihara, M. Meyer, L. Toupet, P. Rabiller, S. Techert, Science, 300 (2003) 612.
[11] R. Neutze, R. Wouts, S. Techert, J. Davidson, M. Kocsis, A. Kirrander, F. Schotte, M. Wulff Phys. Rev. Lett., 87 (2001) 195508.
[12] A. Plech, R. Randler, A. Geis and M. Wulff. J. Synchrotron Rad., 9 (2002) 287.
[13] D. Bourgeois, U. Wagner, M. Wulff, Acta Cryst. D, 56 (2000) 973.
[14] Plech, M. Wulff, S. Bratos, F. Mirloup, R Vuilleumier, F. Schotte and P.A. Anfinrud. submitted.
[15] A.L. Harris, J.K. Brown, and C.B. Harris, Ann. Rev. Phys. Chem., 39 (1988) 341.
[16] J. Tellinghuisen, J. Chem. Phys., 58 (1973) 2821.
[17] D.F. Kelley, A.N. Abul-Haj and D.-J. Jang, J. Chem. Phys., 80 (1984) 4105.
[18] J.T. Hynes, R. Kapral, and G.M. Torrie, J. Chem. Phys., 72 (1980) 177.
[19] F. Hajdu, Acta Cryst. A, 28 (1972) 250.
[20] G. Palinkas, Acta Cryst. A, 29 (1973) 10.
[21] B.E. Warren, X-ray diffraction, chapter 10, Dover, New York, 1969.
[22] A. Khan, J. Chem. Phys., 96 (1992) 1194.